A relative approach for uncertainty quantification of inversely identified material behavior using a heterogeneous test for sheet metal

A relative approach for uncertainty quantification of inversely identified material behavior using a heterogeneous test for sheet metal

M Conde[1], S Coppieters[2] and A Andrade-Campos[1]

[1] Centre for Mechanical Technology and Automation (TEMA), Department of Mechanical Engineering, University of Aveiro, Campus Universitário de Santiago, 3810-193 Aveiro, Portugal

[2] Department of Materials Engineering, KU Leuven, Ghent Technology Campus, Gebroeders De Smetstraat 1, Ghent, 9000, Belgium

E-mail: marianaconde@ua.pt

Abstract. The process of calibrating the material parameters of a constitutive model has inherent uncertainty sources. These can lead to inadequate material behavior characterization and, consequently, errors in the numerical simulations. A robust mechanical test is necessary for accurate material mechanical characterization. In this work, it is relatively quantified the uncertainties of the parameter identification of the Swift hardening law and the Yld2000-2d yield function using Digital Image Correlation (DIC) and a DIC-levelled approach. The levels of uncertainty are calculated with a derivative-based local method, having into consideration the Karush-Kuhn-Tucker (KKT) conditions for optimization problems. The mechanical test used for the parameter calibration was an optimized interior notched specimen that presents several strain and stress states simultaneously. The synthetic images were generated based on the numerical data, and the strain fields were accessed using DIC techniques. It was concluded that the step size is the DIC parameter that most influences the material parameter identification.

1. Introduction, framework and literature review

Nowadays, non-homogeneous mechanical tests came to replace the conventional tests in material mechanical characterization and constitutive parameters identification. These tests, called heterogeneous mechanical tests in this paper, present several strain states simultaneously that can be measured using optical techniques, such as DIC. This large data acquisition can then feed an inverse analysis for parameter identification, such as the Finite Element Model Updating (FEMU) method. Yet, it is of utmost importance to estimate the errors and uncertainties of these identifications. The quantification of the associated errors and the influence of chosen experimental or numerical parameters are essential for parameter identification and, consequently, the accurate simulation and engineering decision making. The DIC procedure alone presents a vast number of sources of uncertainty, namely, the setup misalignment, the sample and camera motion, the air turbulence, the image quality, the setup calibration, the speckle size and shape, the illumination, the image resolution and noise, the aperture, the exposure, the lens distortions, the coordinate system, the correlation for the displacement measurements and the strain and virtual strain gauge (VSG) analysis. Some of these have

been evaluated in [1, 2, 3]. Moreover, the material parameter identification itself produces error propagation since it usually compares experimental data measured with optical techniques and numerical data [4]. So, when using optical cameras to measure displacement fields, it is possible to link image noise to displacement uncertainties, and the latter ones with material parameter fluctuations [5]. Several studies have identified material parameters using FEMU [6, 7, 8, 9, 10]. Also, for model calibration, the Virtual Fields Methods (VFM) is often used, as in [11, 12, 13, 14]. Nevertheless, the vast majority of the mentioned studies did not account for uncertainty measurements in the parameter identification.

The present work aims at quantifying the uncertainties in material parameter identification. Uncertainties in a system can be quantified using probabilistic approaches, such as Monte Carlo simulations, importance sampling, perturbation methods, polynomial chaos expansion (PCE), or non-probabilistic approaches, such as interval analysis and Fuzzy theory [15]. However, the theories and methodologies for uncertainty propagation and inverse uncertainty quantification are computationally expensive and increase dramatically with the dimensionality of the problem (i.e. the number of input variables and/or the number of unknown parameters). Moreover, these suffer from identifiability issues, i.e. multiple combinations of unknown parameters can yield the same prediction, being different parameters indistinguishable. Therefore, knowing that an identification procedure in plasticity can take up to hours, an expedited method is required. Here, considering that the identification problem is solved using optimization techniques and when using virtual experiments the global minimum is known, the KKT conditions [16] can be used for uncertainty quantification and clearness of solution. This approach substantially reduces the computational time.

The identification regarded is a FEMU DIC-levelled technique as in [17], which was already employed with a heterogeneous test in [18]. This FEMU technique compares both the experimental and numerical strain fields using the DIC subset-based method for the strain measurements, minimizing the error between the two. The mechanical test that feeds the FEMU is a heterogeneous test proposed in [19], which was originated by a shape optimization design approach based on a heterogeneity indicator. The constitutive model under consideration is the Swift hardening law and, for the anisotropy behavior, the Yld2000-2d yield function. The sources of uncertainty here analyzed are the subset size, step size and strain window size. Furthermore, the uncertainty technique used is based on the perturbation of the sources of uncertainty and its derivative quantification.

The paper is divided into four main sections. In Section 2, the methodology and implementation, used to quantify the uncertainties of the material parameter identification, are explained in detail. It starts by a simplification of the material calibration problem having in consideration theoretical concepts of optimization problems. The uncertainty technique is described along with (i) the identification problem itself, (ii) the mechanical test in consideration, (iii) the material under analysis, (iv) the simulation and strain calculation and (v) the analyzed sources of uncertainty. In Section 3, the calculated levels of errors in each material parameter and due to each source of uncertainty are presented and discussed. Finally, Section 4 presents the main conclusions.

2. Methodology and implementation

2.1. Uncertainty quantification and problem approach

Model calibration with a large number of material parameters is an optimization problem with a large number of optimization variables that requires severe computational efforts. Furthermore, uncertainty quantification of this type of problem is even more time-consuming. Thus, a simplification of the problem is necessary.

Having into consideration that the identification of material parameters is a non-linear unconstrained optimization problem, the problem's solution satisfies the KKT necessary

conditions [16]. These are first-order necessary conditions for a solution to be optimal. This means that for a cost function f and the optimum solution x^* of the problem, the stationary KKT condition has to be satisfied and can be written as follows:

$$\nabla f(x^*) = 0. \tag{1}$$

In theory, for a continuous cost function f without the presence of noise, these conditions are

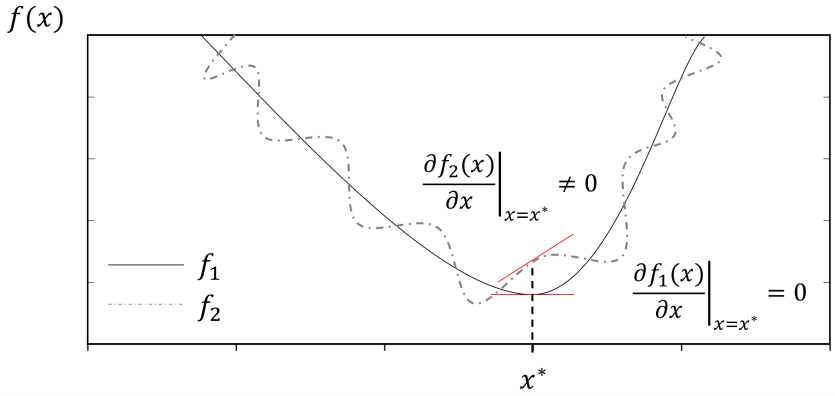

Figure 1. Illustration of the KKT conditions in theory and with a noisy function.

perfectly verified. The partial derivative of the cost function in relation to the optimization variable in the optimal solution is equal to zero (see f_1 in Figure 1). Yet, when f_1 suffers some kind of transformation $f_2 = g(f_1)$ and shows a noisy behavior, the gradient can become different from zero (see f_2 in Figure 1). This transformation is a possible source of errors that must be taken into consideration. Therefore, the level of noise and uncertainties can be evaluated by means of the KKT conditions and it is assumed that the levels of uncertainties increase with the deviation to the KKT conditions.

Assuming that the equality in Equation 1 is verified, it is possible to analyse specific sources of uncertainty. These levels of uncertainty can be estimated with the derivative-based local method that can be written as:

$$\frac{\partial}{\partial \boldsymbol{\theta}}\left(\frac{\partial f}{\partial x}\right), \tag{2}$$

for a $\boldsymbol{\theta}$ representing a vector of analysed sources of uncertainty. Although not yet demonstrated as an accurate method for uncertainty analysis, this approach can be used as a relative method and as a support tool for engineering decision making.

2.2. Identification problem under analysis

The identification approach adopted was the FEMU that is driven by the minimization of the optimization function written as:

$$\varphi(\boldsymbol{\chi}) = \frac{1}{n_\mathrm{t}} \sum_{i=1}^{n_\mathrm{t}} \left\{ \frac{1}{3n_\mathrm{p}} \sum_{j=1}^{n_\mathrm{p}} \left[\left(\frac{\varepsilon_{xx}^{\mathrm{num}}(\boldsymbol{\chi}) - \varepsilon_{xx}^{\mathrm{exp}}}{\varepsilon_{\max}^{\mathrm{exp}}} \right)^2 + \left(\frac{\varepsilon_{yy}^{\mathrm{num}}(\boldsymbol{\chi}) - \varepsilon_{yy}^{\mathrm{exp}}}{\varepsilon_{\max}^{\mathrm{exp}}} \right)^2 + \left(\frac{\varepsilon_{xy}^{\mathrm{num}}(\boldsymbol{\chi}) - \varepsilon_{xy}^{\mathrm{exp}}}{\varepsilon_{\max}^{\mathrm{exp}}} \right)^2 \right]_j + \left(\frac{F^{\mathrm{num}}(\boldsymbol{\chi}) - F^{\mathrm{exp}}}{F_{\max}^{\mathrm{exp}}} \right)^2 \right\}_i, \tag{3}$$

where $\boldsymbol{\chi}$ is the vector of the unknown material parameters, F is the load value and ε are strain components of the mechanical test. The superscripts "num" and "exp" refer to the numerical data obtained iteratively during the optimization process and the experimental data, respectively. The number of time instances is n_t and the number of in-plane measurement points is n_p. $F_\mathrm{max}^\mathrm{exp}$ is the maximum load value and $\varepsilon_\mathrm{max}^\mathrm{exp}$ is the maximum strain value of all in-plane components of the test.

Applying the methodology mentioned in Section 2.1, the partial derivatives of the cost function φ with respect to the material parameters $\boldsymbol{\chi}$ that should satisfy the KKT conditions and Equation 1 can be calculated as:

$$\begin{aligned}\frac{\partial\varphi}{\partial\boldsymbol{\chi}} =& \frac{1}{3n_\mathrm{t}n_\mathrm{p}\cdot(\varepsilon_\mathrm{max}^\mathrm{exp})^2}\sum_{i=1}^{n_\mathrm{t}}\left\{\sum_{j=1}^{n_\mathrm{p}}\left[\left(2\cdot(\varepsilon_{xx}^\mathrm{num}(\boldsymbol{\chi})-\varepsilon_{xx}^\mathrm{exp})\cdot\frac{\partial\varepsilon_{xx}^\mathrm{num}(\boldsymbol{\chi})}{\partial\boldsymbol{\chi}}\right)+\right.\right.\\ &\left.\left.\left(2\cdot(\varepsilon_{yy}^\mathrm{num}(\boldsymbol{\chi})-\varepsilon_{yy}^\mathrm{exp})\cdot\frac{\partial\varepsilon_{yy}^\mathrm{num}(\boldsymbol{\chi})}{\partial\boldsymbol{\chi}}\right)+\left(2\cdot(\varepsilon_{xy}^\mathrm{num}(\boldsymbol{\chi})-\varepsilon_{xy}^\mathrm{exp})\cdot\frac{\partial\varepsilon_{xy}^\mathrm{num}(\boldsymbol{\chi})}{\partial\boldsymbol{\chi}}\right)\right]_j\right\}_i+\\ &\frac{1}{n_\mathrm{t}\cdot(F_\mathrm{max}^\mathrm{exp})^2}\sum_{i=1}^{n_\mathrm{t}}\left(2\cdot(F^\mathrm{num}(\boldsymbol{\chi})-F^\mathrm{exp})\cdot\frac{\partial F^\mathrm{num}(\boldsymbol{\chi})}{\partial\boldsymbol{\chi}}\right)_i,\end{aligned} \tag{4}$$

where the partial derivatives of each numerical strain component $\left(\frac{\partial\varepsilon^\mathrm{num}(\boldsymbol{\chi})}{\partial\boldsymbol{\chi}}\right)$ and of the load value $\left(\frac{\partial F^\mathrm{num}(\boldsymbol{\chi})}{\partial\boldsymbol{\chi}}\right)$ with respect to the material parameters can be quantified using the finite difference method (FDM).

2.3. Heterogeneous mechanical test in consideration

An innovative heterogeneous mechanical test proposed in [20, 19] was the base to generate synthetically deformed images that were used as reference virtual material data in the approach, as well as used for the iterative analysis. The geometry of the heterogeneous specimen is depicted in Figure 2. This interior notched specimen was designed by shape optimization, based on the maximization of the heterogeneity. The heterogeneity of the test was evaluated using several heterogeneity indicators that favor solutions that exhibit several strain states simultaneously with large magnitudes. The shape of the interior notch follows a third-degree spline defined by a total of 20 points. This specimen has 2 symmetries, ensuring the balance during the experimental testing. The specimen is tested under uniaxial loading conditions up to rupture.

2.4. Constitutive model and material definition

Hooke's law was used to describe the linear elastic material behavior of DP600 steel, with a modulus of elasticity of 210 GPa and Poisson's ratio of 0.3. The Swift law [21] was defined for the hardening behavior, and the Yld2000-2d yield criterion [22] for the plastic anisotropy. The reference material parameters used in the virtual experiment of the DP600 steel with 0.8 mm thickness are presented in Table 1. The rupture criterion implemented was based on the FLD (Forming Limit Diagram) [23]. The exponential of the Yld2000-2d function nominated as a is equal to 6 since the material has a BCC type of crystal structure.

2.5. FEA and DIC test simulation: DIC-levelled approach

To model and analyze the heterogeneous mechanical test described in Section 2.3, both the Abaqus [24] and MatchID 2D [25] software were used. A DIC-levelling approach was used to

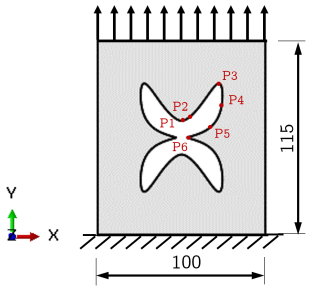

	P1	P2	P3	P4	P5	P6
xx [mm]	0.000	3.708	23.092	23.505	15.889	3.086
yy [mm]	10.000	11.412	31.784	17.078	5.163	0.000

Figure 2. Geometry, dimensions (in mm) and loading conditions of the heterogeneous mechanical test used in the parameter identification approach. Coordinates of the spline considering the origin located in the center of the specimen, in the first quadrant.

Table 1. Reference material parameters of the Swift hardening law and Yld2000-2d yield criterion used for the virtual experiment [23].

Swift law	K [MPa]			ε_0			n		
	979.460			0.00535			0.194		
Yld2000-2d	α_1	α_2	α_3	α_4	α_5	α_6	α_7	α_8	a
	1.011	0.964	1.191	0.995	1.010	1.018	0.977	0.935	6

determine the strain gradients. This was already tested in [4] and implemented in a FEMU method in [17, 18]. First, for the FE analysis, the 2D test was conducted in Abaqus under plane stress state conditions, using 2975 CPS4R elements. The material behavior was implemented using the UMMDp developed by JANCAE (Japan Association of Nonlinear CAE) [26]. A displacement was imposed in the top edge of the specimen, in the vertical direction, up to rupture. The bottom edge of the specimen was kept fixed. A total of 19 time increments presenting elastic and plastic regimes of deformation were used to extract the nodal coordinates and displacements of the mesh. Secondly, these results were used to synthetically deform a speckle pattern to be analyzed using the DIC method. The pattern was numerically generated with 3 px dot size, to avoid aliasing [27] and printed in true dimensions. The hardware and DIC analysis parameters are shown in Table 2. Moreover, a performance analysis was conducted to access the adequate DIC parameters, which are presented in the same table.

2.6. Analyzed sources of uncertainty

Several sources of uncertainty could be evaluated since both the FEA and DIC approaches can influence the outcome of the problem. In the present paper, only the subset size, step size and strain window size were analyzed and discussed. These are the elements of the vector $\boldsymbol{\theta}$ in Equation 2. These are parameters from the DIC analysis that directly influence the strain gradients observed in the specimen and, thus, are very important in parameter identification problems. In order to determine the result of Equation 2, a perturbation of approximately 20 % was applied for each of the parameters that were considered the most suitable for the DIC analysis, after the DIC performance analysis. Although it seems an excessively large value for perturbation to determine the derivatives through the FDM, this is because these DIC parameters are integers that can only vary within specific values and intervals. Therefore, the subset sizes of 21 px and 25 px, the step size of 5 px and 6 px and the strain window size of 11

Table 2. Hardware and DIC analysis parameters using MatchID 2D software [25].

Parameters	
Camera	Flir Blackfly BFS-U3-51S5M-C
Image resolution [px^2]	2448×2048
Focal length [mm]	12.5
Average speckle size [px]	3
Image filtering	Gaussian, 5 px kernel
Image conversion factor [mm/px]	0.07241
Subset size [px]	21
Step size [px]	5
Subset shape function	Quadratic
Matching criterion	ZNSSD
Interpolation	Bi-cubic spline
Strain window [data points]	11
Strain formulation	Green-Lagrange
Post-filtering of strains	Spatial
Displacement noise-floor [px]	0.009
Strain noise-floor [mm/mm]	1.209×10^{-4}

and 13 data points were evaluated.

3. Obtained results and analysis

First, the size of the material parameter perturbation was analyzed in order to better determine the partial derivatives of the FEMU cost function in relation to the material parameters calculated with Equation 4. Perturbation sizes of 10%, 5%, 1% and 0.1% were studied. The results are presented in Figure 3 and they revealed a similar tendency for each parameter. Ideally, a smaller perturbation would be more adequate for the FDM. Though, the 0.1% perturbation shows discrepancies in some anisotropy parameters compared to the other perturbation sizes. Thus, 1% material parameter perturbation was chosen for the following analysis since it is the smaller perturbation that is consistent in relation to the others.

Completing the calculus according to the methodology present in Section 2, with a perturbation of 1 % in the material parameters, it was possible to investigate the influence of each material parameter in the FEMU DIC-levelled problem and the verification of the KKT conditions.

Figure 4 shows the absolute value of the partial derivatives of the cost function with respect to the material parameters (as in Equation 4) in two sets of material parameters. The first is the optimum set of material parameters. Theoretically, its derivatives should be zero, satisfying the KKT conditions. Yet, practically, some of the derivatives are larger than zero. This quantifies the inherent errors caused by the interpolations, transformations, filters and noise and should be accounted for in the interpretation of the following results. The second set of material parameters is obtained randomly. It is presented to understand if the parameter influences the identification process. This is because when starting a FEMU identification, the initial set of material parameters usually is different from the optimum set and each parameter should show influence in the cost function for the optimisation process to flow. If a material parameter is not activated in the mechanical experiment, the value of $\left|\frac{\partial \varphi}{\partial \boldsymbol{\chi}}\right|$ would be zero and the methodology presented could not lead to any conclusions. It can be observed that all the parameters are

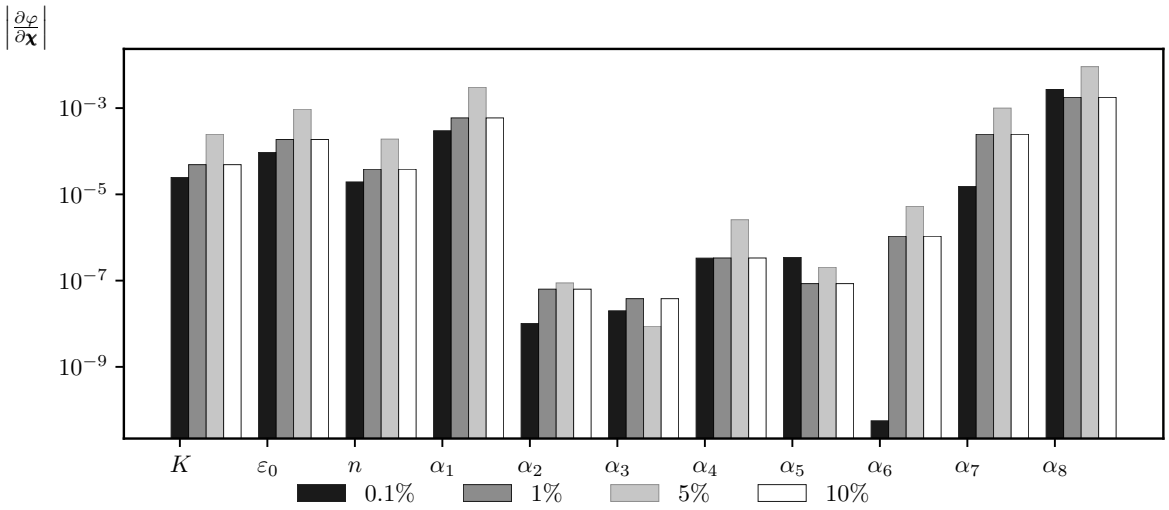

Figure 3. Absolute value of the partial derivatives of the cost function (φ) with respect to the material parameters ($\boldsymbol{\chi}$) with different perturbation sizes.

activated and, thus, influence the identification process. Yet, some present a smaller influence in the FEMU cost function, and, consequently, their derivatives are closer to zero with the optimum set of material parameters. These can present a smaller sensitivity in the methodology. The material parameters of the random set can be observed in Table 3.

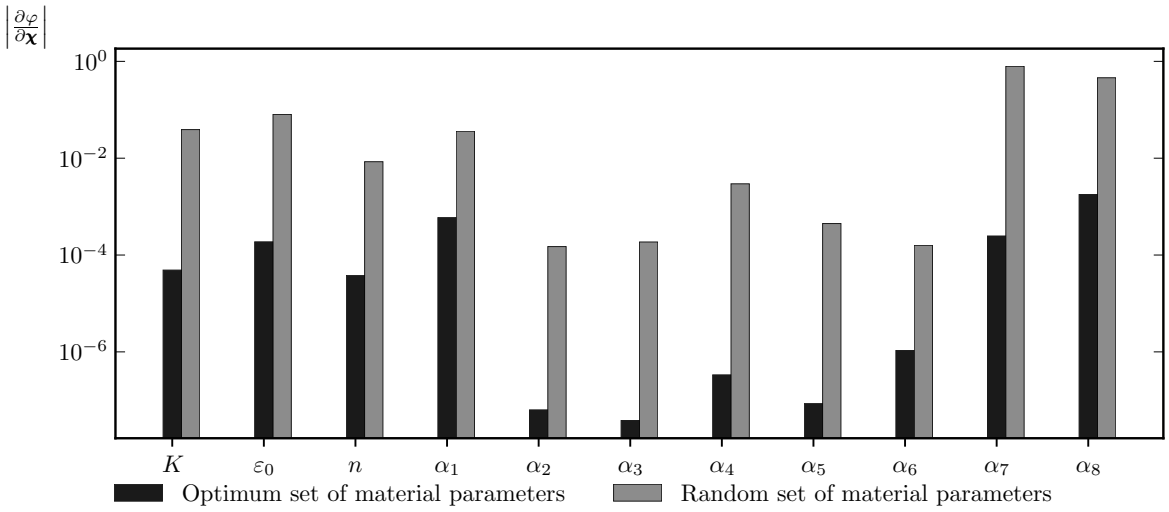

Figure 4. Absolute value of the partial derivatives of the cost function (φ) with respect to the material parameters ($\boldsymbol{\chi}$) in the optimum and random sets of parameters.

The influence of each source of uncertainty in the problem can be seen in Figure 5. It can be stated that α_7 and α_8 are more sensitive to uncertainties. This can be both from the propagation of errors that are observed in Figure 4 and from the influence of each studied source of uncertainty (subset, step and strain window sizes). Furthermore, the step size is the analyzed source of uncertainty that largest influences the FEMU DIC-levelled parameter identification.

Table 3. Random set of material parameters of the Swift hardening law and Yld200-2d yield criterion used to determine $\left|\frac{\partial\varphi}{\partial\boldsymbol{\chi}}\right|$ in Figure 4.

Swift law	K [MPa]			ε_0			n		
	960.511			0.00559			0.189		
Yld2000-2d	α_1	α_2	α_3	α_4	α_5	α_6	α_7	α_8	a
	1.123	1.310	0.899	0.905	0.974	1.200	1.076	0.869	6

The subset and strain window sizes have a similar impact on the problem and in the search for the identification solution.

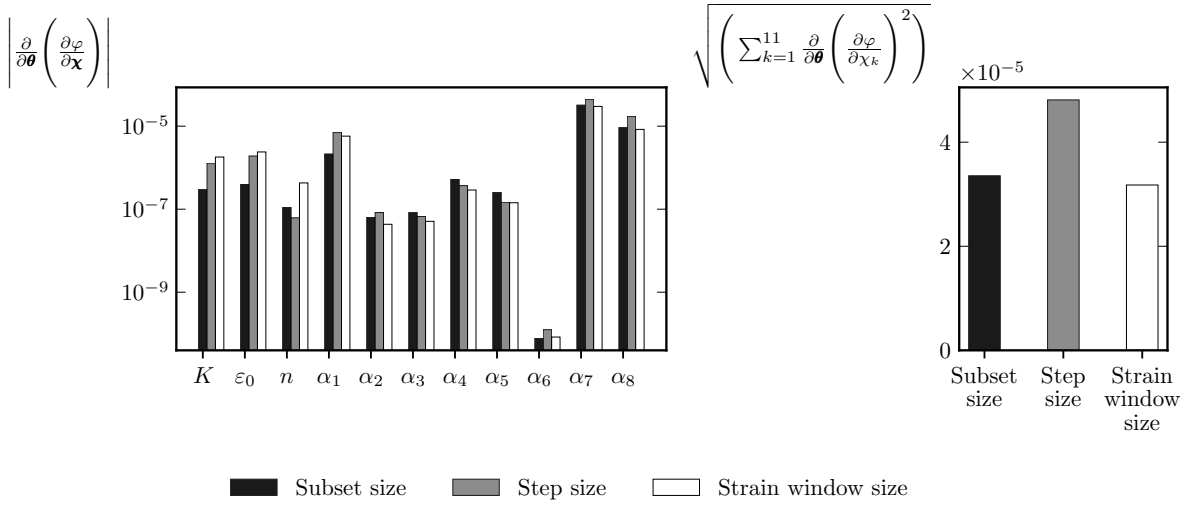

Figure 5. Influence of the subset size, step size and strain window size in each material parameter and in the overall parameter identification approach.

4. Main conclusions

In the present paper, a methodology was developed to quantify the uncertainties in material parameter identification, using the assumptions of the KKT necessary conditions of non-linear unconstrained optimization problems. This way it was possible to simplify the identification problem and estimate the uncertainties with less computational effort, leading to faster engineering decision making. The calibration problem considered was the FEMU DIC-levelled approach and the uncertainty technique was the derivative-based local method by means of the finite difference method. The mechanical test used in the inverse identification process was an interior notched specimen for uniaxial loading conditions that presents several strain and stress states simultaneously. The calibration of the Swift hardening law and Yld2000-2d yield function was evaluated. The sources of uncertainty analyzed were the subset, step and strain window sizes.

It was concluded that the obtained errors in the material parameter identification using a FEMU DIC-levelled technique were originated by the propagation of errors of the measurements, interpolation and discretization of the problem itself and from the influence of the sources of uncertainty. Moreover, the step size has a larger impact on the identified material parameters,

compared to the subset size and strain window size for the studied speckle pattern and strain gradients. Special attention must be paid when choosing the DIC settings for an inverse identification of material parameters since they have a direct effect on the strain gradients and measurements and also a different impact in the inverse identification of the material parameters.

Acknowledgments

This project has received funding from the Research Fund for Coal and Steel under grant agreement No 888153. The authors also acknowledge the financial support of the Portuguese Foundation for Science and Technology (FCT) under the project PTDC/EME-APL/29713/2017 by UE/FEDER through the programs CENTRO 2020 and COMPETE 2020, and UID/EMS/00481/2013-FCT under CENTRO-01-0145-FEDER-022083. Mariana Conde is grateful to the Portuguese Foundation for Science and Technology (FCT) for the PhD grant 2021.06115.BD.

References

[1] Lava P, Coppieters S, Wang Y and Houtte P V 2011 *Applied Mechanics and Materials* **70** 165–170
[2] Lava P, Coppieters S, Wang Y, Houtte P V and Debruyne D 2011 *Optics and Lasers in Engineering* **49** 57–65 ISSN 0143-8166
[3] Rossi M, Lava P, Pierron F, Debruyne D and Sasso M 2015 *Strain* **51** 206–222 ISSN 14751305
[4] Lava P, Jones E M C, Wittevrongel L and Pierron F 2020 *Strain* **56**
[5] Roux S and Hild F 2020 *International Journal of Solids and Structures* **184** 14–23
[6] Haddadi H and Belhabib S 2012 *International Journal of Mechanical Sciences* **62** 47–56 ISSN 00207403
[7] Peixoto J, Andrade-campos A and Thuillier S 2020 Calibration of Johnson-Cook Model Using Heterogeneous Thermo- Mechanical Tests *Procedia Manufacturing* vol 47 (Elsevier B.V.) pp 881–888 ISBN 3512343708 ISSN 2351-9789
[8] Pereira A F G, Prates P A, Sakharova N A, Oliveira M C and Fernandes J V 2014 *Engineering with Computers*
[9] Pottier T, Toussaint F and Vacher P 2011 *European Journal of Mechanics, A/Solids* **30** 373–382 ISSN 09977538
[10] Souto N, Andrade-campos A and Thuillier S 2015 *Journal of Materials Processing Tech.* **220** 157–172 ISSN 0924-0136
[11] Martins J M P, Andrade-campos A and Thuillier S 2019 *International Journal of Solids and Structures* **172-173** 21–37 ISSN 0020-7683
[12] Jones E M, Carroll J D, Karlson K N, Kramer S L, Lehoucq R B, Reu P L and Turner D Z 2018 *Computational Materials Science* **152** 268–290 ISSN 09270256
[13] Wang P, Pierron F, Rossi M, Lava P and Thomsen O 2015 *Strain* 1–44
[14] Zhang S, Xing T, Zhu H and Chen X 2020 *Materials* **13** 1–12 ISSN 19961944
[15] Christian S 2017 *Uncertainty Quantification* 1st ed (Springer, Cham) ISBN 978-3-319-54338-3
[16] Kuhn H and Tucker A 1956 *Princeton University Press, Princeton, NJ*
[17] Henriques J, Conde M, Andrade-Campos A and Xavier J 2022 Identification of Swift law parameters using FEMU by a synthetic image approach based on digital image correlation *Esaform 2022 - 25th International Conference on Material Forming* (Braga, Portugal)
[18] Conde M, Henriques J, Coppieters S and Andrade-Campos A 2022 Parameter identification of Swift law using a FEMU-based approach and an innovative heterogeneous mechanical test *Esaform 2022 - 25th International Conference on Material Forming* (Braga, Portugal)
[19] Conde M, Andrade-Campos A, Oliveira M G and Martins J M P 2021 Design of heterogeneous interior notched specimens for material mechanical characterization *Esaform 2021 - 24th International Conference on Material Forming* (Liège, Belgique)
[20] Conde M 2020 *Design of a heterogeneous interior notched specimen using shape optimisation approach* Masters thesis University of Aveiro, Portugal
[21] Swift H W 1952 *Journal of the Mechanics and Physics of Solids* **1** 1–18
[22] Barlat F, Brem J C, Yoon J W, Chung K and Dick R E 2003 *International Journal of Plasticity* **19** 1297–1319
[23] Ozturk F, Toros S and Kilic S 2014 Effects of anisotropic yield functions on prediction of forming limit diagrams of DP600 advanced high strength steel *Procedia Engineering* vol 81 (Elsevier B.V.) pp 760–765 ISSN 18777058
[24] Dassault Systèmes 2014 Abaqus 6.14 Online Documentation

[25] MatchID 2021 New MatchID release 2021.1
[26] Takizawa H, Kuwabara T, Oide K and Yoshida J 2016 Development of the subroutine library 'UMMDp' for anisotropic yield functions commonly applicable to commercial FEM codes *Journal of Physics: Conference Series* vol 734 ISSN 17426596
[27] International Digital Image Correlation Society, Jones E and Iadicola M 2018 *A Good Practices Guide for Digital Image Correlation*